Brookhaven National Laboratory

U.S. DEPARTMENT OF ENERGY

Tables of Neutron Thermal Cross Sections, Westcott Factors, Resonance Integrals, Maxwellian Averaged Cross Sections, Astrophysical Reaction Rates, and r-process Abundances Calculated from the ENDF/B-VIII.1, JEFF-3.3, JENDL-5.0, BROND-3.1, and CENDL-3.2 Evaluated Data Libraries

Boris Pritychenko

National Nuclear Data Center, Brookhaven National Laboratory, Upton, NY 11973-5000, USA

December 4, 2024

Compilation of Experimental Nuclear Reaction Data

ENDF/B-VIII.1Library Release

- The CSEWG collaboration released the ENDF/B-VIII.1 library in FY 2024—many details are in G. Nobre's (BNL) presentation.

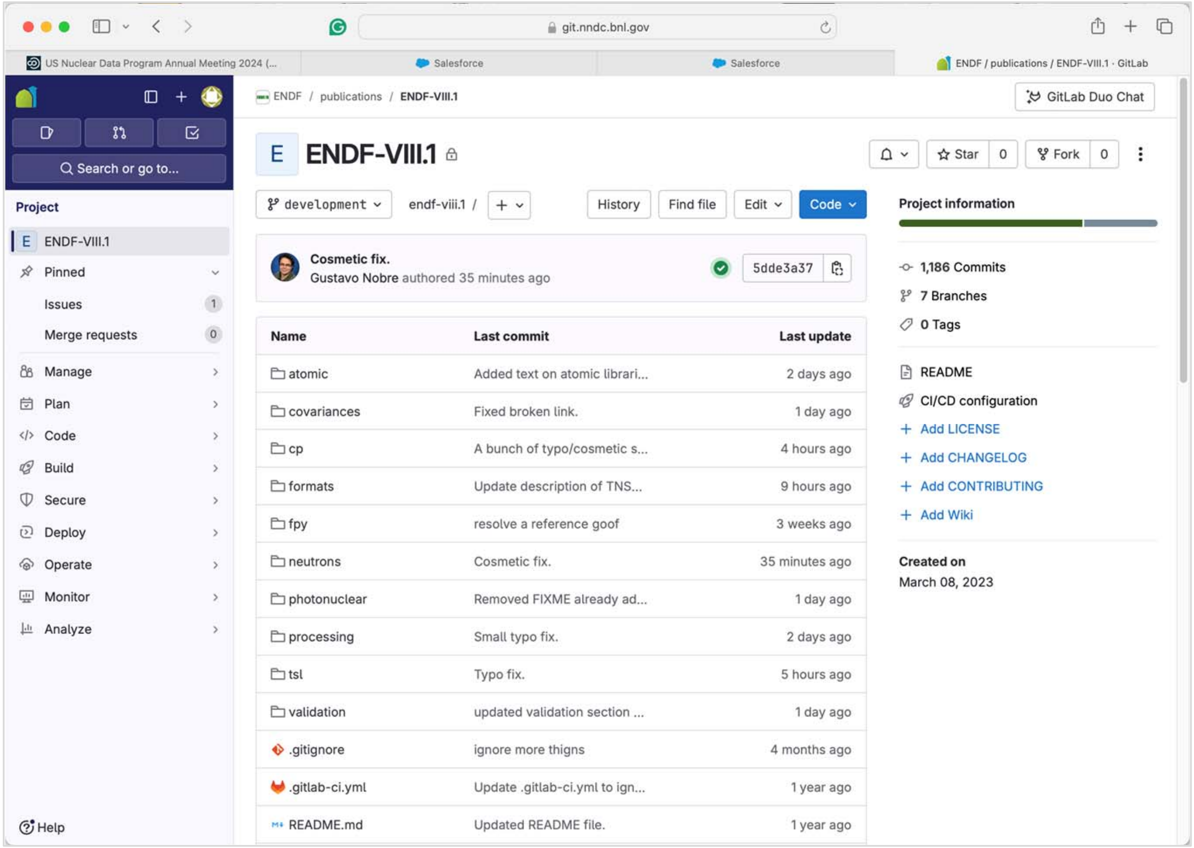

ENFG/B-VIII.1 Integral Values

- For the ENDF/B-VIII.1 library validation purposes, Neutron Thermal Cross Sections, Westcott Factors, Resonance Integrals, Maxwellian Averaged Cross Sections, Astrophysical Reaction Rates, and r-process Abundances were calculated.
- The calculation was extended to JEFF-3.3, JENDL-5.0, CENDL-3.2, and BROND-3.1 libraries.
- We Doppler-broaden evaluated reaction data at 293.16 $\circ$ K and extracted thermal cross sections for (n,γ), (n,fission), and (n,el) from the libraries.
- Results were compared with the Atlas of Neutron Resonances (2018), ASTRAL and EXFOR libraries.

Unified Neutron Material Grid

- How many neutron materials are in the five major libraries: 849.
- How materials are present in all libraries: 254.
- The 254 common neutron materials

are present in the neutron sublibraries of the five libraries. The shown below list of common 254 neutron targets illustrates comprehensive nuclear reaction evaluation efforts around the globe and explains the interest in the evaluated data sets for multiple applications: $^{1-3}$H, ^{3,4}He, ^{6,7}Li, ^{9}Be, ^{10,11}B, C/^{12,13}C, ^{14}N, ^{16}O, ^{19}F, ^{23}Na, $^{24-26}$Mg, ^{27}Al, $^{28-30}$Si, ^{31}P, $^{32-34,36}$S, Cl/^{35,37}Cl, K/$^{39-41}$K, Ca/^{40}Ca, $^{46-50}$Ti, V/^{50,51}V, $^{50,52-54}$Cr, ^{55}Mn, $^{54,56-58}$Fe, ^{59}Co, $^{58,60-62,64}$Ni, ^{63,65}Cu, $^{64,66-68,70}$Zn, ^{69,71}Ga, $^{70,72-74,76}$Ge, ^{75}As, $^{76-80,82}$Se, $^{83-86}$Kr, $^{85-87}$Rb, $^{88-90}$Sr, ^{89,91}Y, $^{90-96}$Zr, ^{93,95}Nb, $^{92,94-100}$Mo, ^{99}Tc, $^{99-105}$Ru, ^{103,105}Rh, ^{105,108}Pd, ^{107,109}Ag, Cd/^{113}Cd, ^{113,115}In, $^{112,114-120,122,124,126}$Sn, $^{121,123-125}$Sb, ^{130}Te, $^{127,129-131,135}$I, $^{129,131-136}$Xe, $^{133-135,137}$Cs, $^{130,132,134-138}$Ba, ^{139}La, $^{136,138,140-142,144}$Ce, ^{141}Pr, $^{142-148,150}$Nd, $^{147-149}$Pm, $^{144,147-152,154}$Sm, $^{151,153-155}$Eu, $^{152,154-158,160}$Gd, ^{164}Dy, ^{165}Ho, $^{174,176-180}$Hf, ^{181}Ta, $^{180,182-184,186}$W, ^{197}Au, $^{204,206-208}$Pb, ^{209}Bi, ^{232}Th, $^{232-238,240}$U, $^{236-239}$Np, $^{236-242,244,246}$Pu, and $^{241-243}$Am. The analysis of common target materials shows that the national libraries provide recommended values for stable and long-lived radioactive nuclei. Far

Westcott Factors

- Westcott factors

Westcott g-factor, g_w, is the ratio of Maxwellian-averaged cross section to the 2200 m/s (thermal) cross section [41, 42]

$$g_w = \frac{\sigma^{Maxw}}{\sigma^{2200}}, \tag{1}$$

or

$$g_w = \frac{\sigma^{Maxw}}{\sigma^{2200}} = \frac{4}{\upsilon_0 \sigma_0 \sqrt{\pi}} \int_0^\infty \frac{\upsilon^3}{\upsilon_T^3} e^{-(\frac{\upsilon}{\upsilon_T})^2} \sigma(\upsilon) d\upsilon, \tag{2}$$

where υ_0 (2200 m/sec) is the velocity of a neutron of energy kT_0 with $T_0 = 293.60°$ K (20.44° C), and $\upsilon_T = \upsilon_0 \sqrt{\frac{T}{T_0}}$ [42].

- Large Westcott factors >2 indicate spectra merging issues in ENDF libraries.
- Elastic Westcott factors ~1.12, consistent with the 2012 calculation.
- In the Atlas, we notice several typos in the reference book where neutron capture factors for ^{59}Ni, ^{141}Ce, ^{152}Gd, $^{160-161}$Dy, ^{168}Er, and ^{173}Lu are not displayed correctly.

Brookhaven National Laboratory

Resonance Integrals (RI)

- They are defined by Lamarsh in a quasi-physical interpretation as “...the resonance integral is equal to the integral of the [effective] absorption [capture] cross section over the resonance region which is necessary to account for the observed neutron absorption rate in a flux equal to that existing in the absence of the resonances.”

$$RI = \int_{E_c}^{\infty} \sigma_R(E) \frac{dE}{E}$$

- The integrals for (n,γ), (n, fission), and (n, el) were calculated and compared with the Atlas of Neutron Resonances (2018).

Maxwellian-Averaged Cross Sections (MACS)

- Fission and capture MACS were calculated for *kT*=8, 25, 30, 90, and 1420 keV

$$\sigma^{Maxw}(kT) = \frac{2}{\sqrt{\pi}} \frac{a^2}{(kT)^2} \int_0^\infty \sigma(E_n^L) E_n^L e^{-\frac{aE_n^L}{kT}} \, dE_n^L$$

- Capture *kT*=30 keV values are listed in the ENDF/B-VIII.1 paper.
- The ASTRAL library is used for comparative purposes: *https://exp-astro.de/astral/.*
- Astrophysical reaction rates were calculated for the five temperatures

$$R(T_9) = 10^{-24} N_A \sigma^{Maxw}(kT) \upsilon_T$$

B Maxwellian-averaged Cross Sections — I INTEGRAL QUANTITIES IN ENDF/B-VIII.1

TABLE III: ENDF/B-VIII.0, ENDF/B-VIII.1, JENDL-5, JEFF-3.3, and ASTRAL Maxwellian-averaged neutron capture cross sections and their ratios at *kT*=30 keV.

Material	ENDF/B-VIII.0 (barns)	ENDF/B-VIII.1 (barns)	JENDL-5 (barns)	JEFF-3.3 (barns)	ASTRAL (barns)	ASTRAL/ENDF/B-VIII.1
1-H - 1	1.544E-4±8.865E-6	1.544E-4±8.865E-6	1.544E-4±8.865E-6	1.559E-4±5.890E-6		
1-H - 2	1.980E-6±1.236E-7	1.980E-6±1.236E-7	2.345E-6	1.972E-6±3.943E-7		
1-H - 3						
2-He- 3	2.109E-5	2.109E-5	1.629E-5	2.109E-5		
2-He- 4						
3-Li- 6	3.290E-5	3.290E-5	3.346E-5	3.290E-5±3.180E-6		
3-Li- 7	4.663E-5	4.663E-5	3.917E-5	4.663E-5		
4-Be- 7			4.341E-5			
4-Be- 9	9.324E-6±1.860E-6	1.074E-5±2.143E-6	7.424E-6	1.270E-5±3.235E-6	9.079E-6±4.273E-7	8.457E-1±2.051E-1
5-B - 10	3.440E-4±2.752E-4	3.440E-4±2.752E-4	4.393E-4±1.757E-4	4.311E-4±3.449E-4		
5-B - 11	6.620E-5±2.047E-5	6.620E-5±2.047E-5	5.669E-5±1.733E-5	6.620E-5±2.047E-5		
6-C - 12	1.557E-5±3.112E-6	1.557E-5±3.112E-6	1.583E-5			
6-C - 13	1.736E-5	1.736E-5	2.893E-5±8.927E-138	1.385E-5±1.990E-95	2.812E-5±6.454E-6	1.620E+0±2.295E-1
7-N - 14	6.696E-5	6.696E-5	6.753E-5	6.696E-5		
7-N - 15	9.175E-6±4.587E-6	9.175E-6±4.587E-6	7.104E-6	9.175E-6±4.587E-6		
8-O - 16	3.637E-5±3.639E-6	3.637E-5±3.639E-6	3.149E-5±3.186E-6	3.149E-5±3.158E-6		
8-O - 17	4.695E-6	4.695E-6	1.964E-5	3.693E-6±7.026E-8		
8-O - 18	1.716E-7	2.894E-6	6.550E-5	4.881E-4±5.591E-17		
9-F - 19	4.372E-3±1.817E-4	5.730E-3±2.367E-4	5.729E-3	4.372E-3		
10-Ne- 20	1.180E-4±4.125E-29	1.180E-4±4.125E-29	3.201E-4	1.180E-4±4.125E-29		
10-Ne- 21	2.261E-3±6.993E-6	2.261E-3±6.993E-6	8.984E-4	2.261E-3±6.993E-6		
10-Ne- 22	8.373E-5±6.524E-21	8.371E-5±6.524E-21	5.693E-6	8.371E-5±6.524E-21		
11-Na- 22	8.019E-3	8.016E-3	3.127E-3	2.744E+0±2.598E-4		
11-Na- 23	1.832E-3±1.371E-4	1.832E-3±1.371E-4	1.555E-3±1.642E-4	2.048E-3±4.687E-4	1.519E-3±1.399E-5	8.289E-1±7.540E-2
12-Mg- 24	3.789E-3±7.179E-4	3.789E-3±7.178E-4	3.789E-3	3.789E-3±4.996E-6		
12-Mg- 25	5.280E-3±1.305E-6	5.279E-3±1.305E-6	5.279E-3	5.279E-3±4.120E-4		
12-Mg- 26	8.610E-5±1.617E-5	8.609E-5±1.617E-5	8.609E-5	8.609E-5±5.477E-6		
13-Al- 26M	4.362E-3	4.361E-3				
13-Al- 27	3.307E-3±5.612E-4	3.307E-3±5.612E-4	3.337E-3	3.307E-3±2.710E-14		
14-Si- 28	3.607E-3±8.000E-4	1.326E-3±2.857E-4	3.607E-3	3.607E-3		
14-Si- 29	7.772E-3±8.349E-4	6.624E-3±7.146E-4	7.771E-3	7.771E-3±8.348E-4		
14-Si- 30	4.448E-3±1.520E-3	1.415E-3±2.324E-4	4.447E-3	4.447E-3±1.520E-3		
14-Si- 31	1.405E-2	1.405E-2	4.919E-4	3.590E-4±9.528E-12		
14-Si- 32	1.245E-4	1.245E-4	4.529E-5	1.245E-4±2.163E-13		
15-P - 31	7.240E-3	7.240E-3	1.627E-3	2.095E-3±2.286E-9		
16-S - 32	5.660E-3	5.660E-3	5.660E-3	5.817E-3±1.629E-25		
16-S - 33	2.277E-3	2.277E-3	2.277E-3	5.818E-3±2.793E-11		
16-S - 34	2.324E-4	2.324E-4	2.324E-4	3.119E-4±1.641E-27	8.087E-4±3.202E-5	3.481E+0±3.959E-2
16-S - 35	6.363E-4	6.363E-4	2.172E-3	6.105E-4±1.757E-6		
16-S - 36	6.331E-4	6.331E-4	6.331E-4	2.318E-3±8.860E-19		
17-Cl- 35	7.541E-3	7.540E-3	7.540E-3	7.540E-3		
17-Cl- 36	1.172E-2	1.172E-2	6.394E-3	7.010E-3±2.911E-3		
17-Cl- 37	2.043E-3	2.043E-3	2.043E-3	2.043E-3		
18-Ar- 36	8.842E-3	8.842E-3	5.143E-3	8.291E-3±4.810E-10	1.524E-3±1.067E-4	1.724E-1±7.000E-2
18-Ar- 37	1.020E-2±1.191E-3	1.020E-2±1.191E-3	1.247E-2	1.020E-2±1.191E-3		
18-Ar- 38	1.365E-4	1.365E-4	8.679E-4	2.754E-3±1.387E-10	9.336E-4±1.027E-4	6.837E+0±1.100E-1
18-Ar- 39	1.992E-2	1.992E-2	1.146E-2	4.947E-3±7.328E-5		
18-Ar- 40	2.248E-3	2.248E-3	2.248E-3	2.248E-3		
18-Ar- 41	2.579E-2±1.241E-2	2.579E-2±1.241E-2	6.736E-3	2.579E-2±1.241E-2		
19-K - 39	1.057E-2	1.057E-2	1.057E-2	1.029E-2±9.207E-20		
19-K - 40	1.941E-2	1.941E-2	3.264E-2	2.915E-2±1.506E-2		
19-K - 41	2.031E-2±1.057E-16	2.031E-2±1.057E-16	2.031E-2	1.988E-2±4.411E-16		
20-Ca- 40	9.972E-3	9.971E-3	5.146E-3	5.464E-3±6.614E-23	5.159E-3±3.044E-4	5.174E-1±5.900E-2
20-Ca- 41	3.854E-2	3.854E-2	2.243E-2	3.827E-2±3.168E-3		
20-Ca- 42	1.241E-2	1.241E-2	1.241E-2	1.315E-2±6.169E-10		
20-Ca- 43	3.530E-2	3.530E-2	3.804E-2	6.897E-2±1.276E-4		
20-Ca- 44	7.744E-3	7.744E-3	7.744E-3	7.634E-3±3.190E-10		
20-Ca- 45	2.025E-2±8.270E-3	2.025E-2±8.270E-3	1.470E-2	2.025E-2±8.270E-3		
20-Ca- 46	1.860E-3	1.860E-3	2.590E-3	6.268E-3±1.401E-6		
20-Ca- 47	9.064E-3±3.097E-4	9.064E-3±3.097E-4	2.942E-3	9.064E-3±3.097E-4		
20-Ca- 48	1.080E-4	1.080E-4	1.080E-4	8.617E-4±5.116E-44		
21-Sc- 45	6.840E-2	6.840E-2	6.555E-2	6.452E-2±1.061E-3	5.530E-2±6.107E-4	8.084E-1±1.105E-2
22-Ti- 46	2.545E-2±1.209E-7	2.545E-2±1.209E-7	2.545E-2	2.603E-2±1.006E-6		
22-Ti- 47	4.868E-2±1.449E-3	4.868E-2±1.449E-3	4.665E-2	5.828E-2±5.937E-3		
22-Ti- 48	2.656E-2±7.043E-9	2.656E-2±7.043E-9	2.656E-2±2.205E-8	2.656E-2±8.983E-8		
22-Ti- 49	1.583E-2±2.961E-6	1.583E-2±2.961E-6	1.583E-2	1.321E-2±1.032E-5		
22-Ti- 50	3.044E-3±8.050E-12	3.044E-3±8.050E-12	3.044E-3	3.433E-3±2.447E-24		
23-V - 49	1.475E-1	1.475E-1	6.849E-2	2.338E-1±1.108E-1		
23-V - 50	2.132E-2	2.132E-2	2.132E-2	4.322E-2±6.376E-4		
23-V - 51	3.205E-2	2.613E-2±1.476E-5	3.196E-2	3.169E-2±1.302E-5		
24-Cr- 50	3.828E-2	4.506E-2	3.828E-2	3.828E-2±3.828E-6		
24-Cr- 51	8.450E-2±2.707E-2	8.428E-2	6.330E-2	8.449E-2±2.707E-2		
24-Cr- 52	7.992E-3±2.709E-4	8.996E-3±3.060E-4	7.991E-3±1.534E-22	7.991E-3		
24-Cr- 53	2.598E-2	5.179E-2	2.620E-2±6.296E-10	2.598E-2±2.598E-6		
24-Cr- 54	4.780E-3	4.780E-3	4.780E-3	4.780E-3±4.780E-7		
25-Mn- 54	2.449E-1±1.387E-1	2.449E-1±1.387E-1	9.318E-2	2.449E-1±1.387E-1		
25-Mn- 55	3.284E-2±2.666E-3	3.284E-2±2.666E-3	3.255E-2±2.846E-3	3.293E-2±2.817E-3		
26-Fe- 54	2.715E-2±4.934E-3	2.981E-2±5.419E-3	2.715E-2	2.160E-2		
26-Fe- 55	9.097E-2±1.895E-2	9.096E-2±1.895E-2	7.563E-2	9.096E-2±1.895E-2		
26-Fe- 56	1.355E-2±4.774E-4	1.262E-2±4.382E-4	1.257E-2±1.236E-3	1.148E-2±1.607E-3		
26-Fe- 57	3.601E-2	3.601E-2	3.601E-2	3.027E-2		
26-Fe- 58	1.507E-2	1.506E-2	1.506E-2±4.450E-8	1.506E-2	1.258E-2±3.394E-4	8.350E-1±2.699E-2
27-Co- 58	2.107E-1	2.107E-1	1.077E-1	2.864E-1±1.345E-1		
27-Co- 58M	6.449E-2	6.449E-2	2.034E-1	1.176E+0±7.265E-2		
27-Co- 59	3.426E-2	3.426E-2	3.422E-2±5.560E-3	3.444E-2	3.554E-2±2.051E-4	1.037E+0±5.771E-3
28-Ni- 58	3.387E-2±2.776E-3	3.387E-2±2.775E-3	3.387E-2±1.591E-13	4.002E-2±5.325E-10		
28-Ni- 59	5.102E-2	5.102E-2	9.783E-2	8.681E-2±7.840E-2		
28-Ni- 60	2.677E-2±1.594E-3	2.677E-2±1.593E-3	2.677E-2±1.757E-13	2.826E-2±7.336E-10		
28-Ni- 61	9.307E-2	9.306E-2	8.915E-2	9.033E-2		
28-Ni- 62	2.384E-2	2.383E-2	2.383E-2	1.925E-2±6.518E-10		
28-Ni- 63	5.109E-2	5.109E-2	4.995E-2	2.930E-2±2.391E-2		
28-Ni- 64	2.007E-2	2.007E-2	2.007E-2	2.007E-2	7.108E-3±1.586E-4	3.542E-1±2.231E-2
29-Cu- 63	5.930E-2	7.283E-2	7.319E-2	7.141E-2±2.304E-3		
29-Cu- 64	1.506E-1	1.506E-1	1.163E-1	2.630E-1±9.663E-2		
29-Cu- 65	3.380E-2	3.480E-2	3.854E-2	3.890E-2±1.313E-3	2.696E-2±7.097E-4	7.748E-1±2.632E-2

JENDL-5.0 Fission MACS

- JENDL-5.0 has non-zero fission cross sections for ^{205}Pb above 20 MeV, and no experimental data in EXFOR.
- As a result, MACS of 1.569E-296 barns is calculated for *kT* =30 keV, 7.641E-105 b for *kT*=90 keV, and 2.331E-14 b at *kT*=1420 keV.
- The *kT*=1420 keV value is larger than superheavy element production cross section but smaller than the neutrino interaction.
- A similar situation is also observed in ^{211,222}Rn, where fission starts from 6.5 and 4 MeV, respectively.

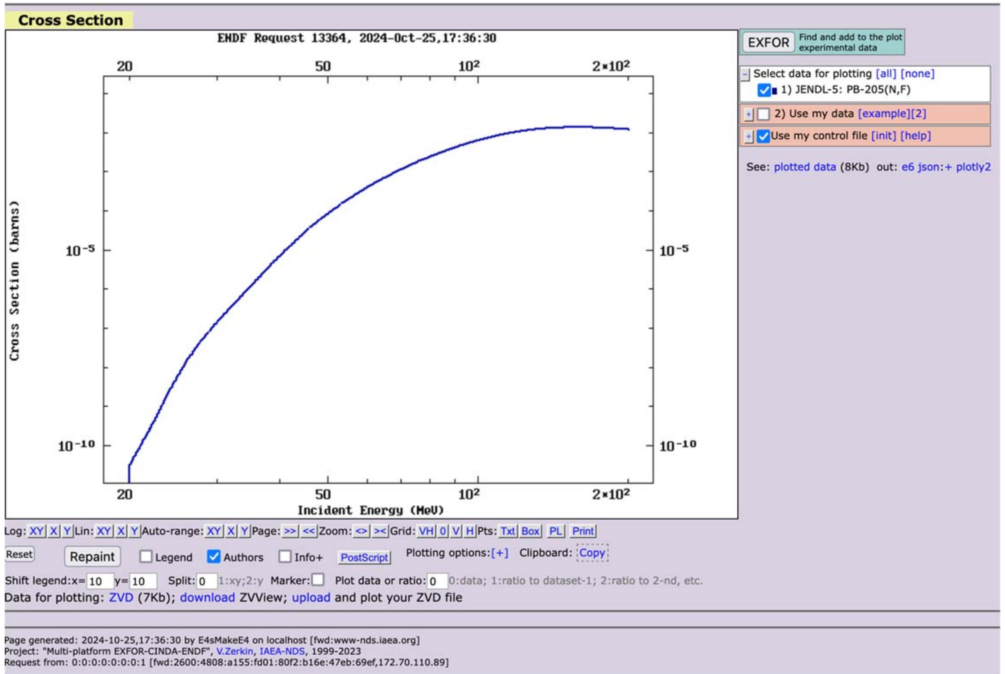

Comparison of ENDF/B-VIII.1 and ASTRAL MACS

- The analysis of the ratios shows agreements in most cases and strong deviations in ^{13}C, ^{34}S, ^{36,38}Ar, and ^{196}Hg and minor deviations in ^{40}Ca, ^{64}Ni, ^{120}Te, and ^{126,129}Xe cases.
- The analysis of the EXFOR database shows that there are no experimental data for ^{36,38}Ar and ^{126}Xe above thermal region, and the observed differences are due to the issues with theoretical modeling.
- In cases of ^{129}Xe and ^{196}Hg, ASTRAL results are based on single measurements that could be deficient.
- In ^{40}Ca we need to consider three contradictory measurements and choices of ENDF and ASTRAL evaluators.

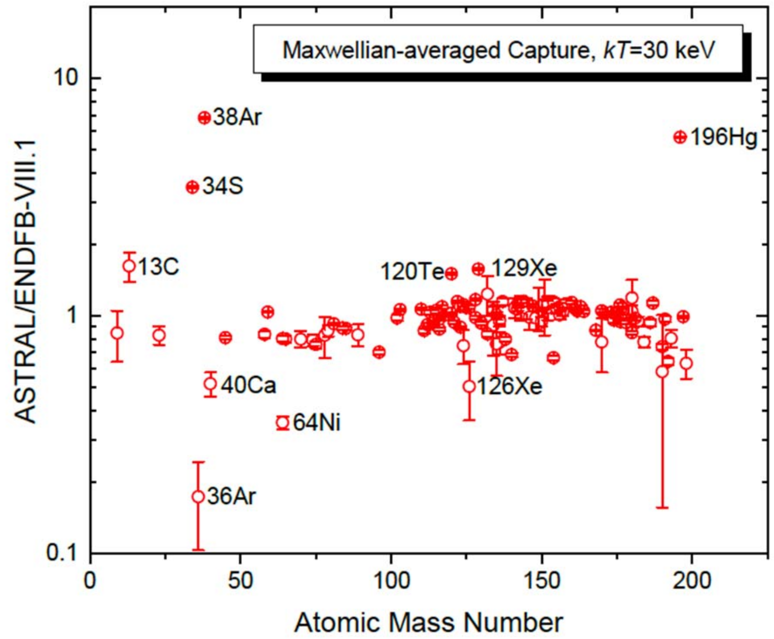

Brookhaven National Laboratory

s-Process

- Slow-neutron capture (*s*-process) is reasonably well understood. It starts from 56Fe and follows the valley of stability.
- σN systematics for equilibrium conditions in AGB stars

$$\sigma_{(A)} N_{(A)} = \frac{f N_{56}}{\tau_0} \prod_{i=56}^{A} \left[1 + \frac{1}{\sigma(i)\tau_0}\right]^{-1}$$

- The total ENDF/B-VIII.1 values include *s*- and *r*- (rapid neutron capture) processes.

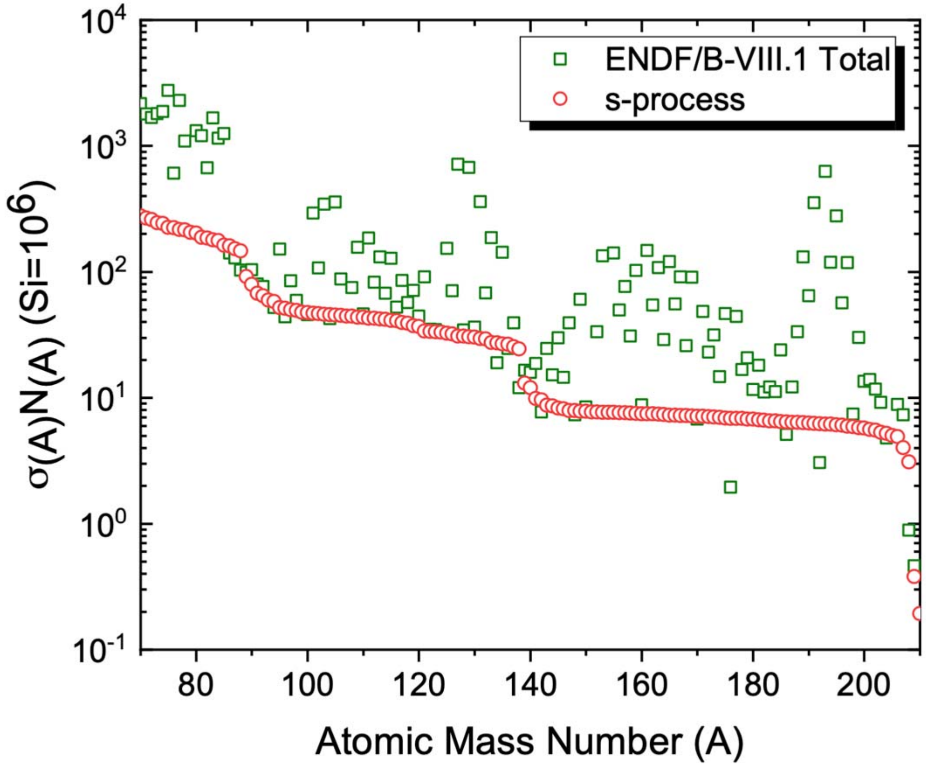

ENDF/B-VIII.1 r-process Abundances

- The r-process abundances were extracted using ENDF/B-VIII.1 Maxwellian-averaged Cross Sections and Solar system abundances.
- Results agree well with Arlandini et al., and Arnould et al.
- In ENDF/B-VIII.0 we had issues with ^{138}Ba and ^{140}Ce abundances.
- ^{140}Ce in ENDF/B-VIII.1 is good.

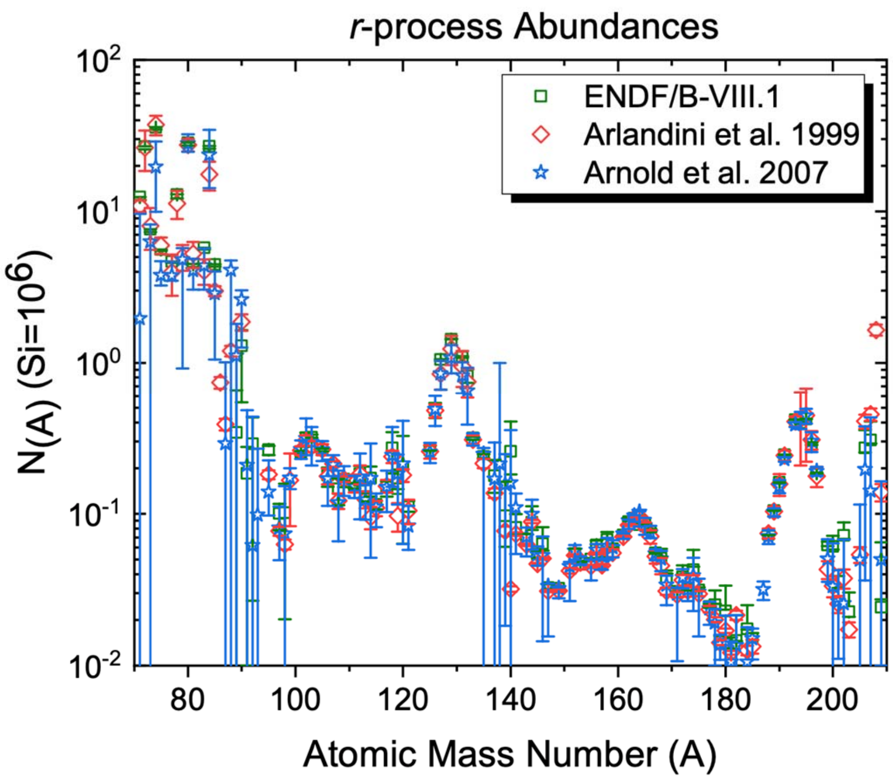

Brookhaven National Laboratory

ENDF/B-VIII.1, JEFF-3.3, and JENDL-5.0 r-Process Abundances

- Calculation was extended to JEFF-3.3 and JENDL-5.0 libraries.
- JEFF/JENDL have issues with ^{138}Ba and ^{140}Ce abundances.
- CENDL-3.2, and BROND-3.1 do not have a sufficient number of target nuclei for the s-process.
- Results are comparable with ENDF/B-VIII.1; however, cerium evaluation in ENDF/B-VIII.1 provides a clear preference for the ENDF/B library.

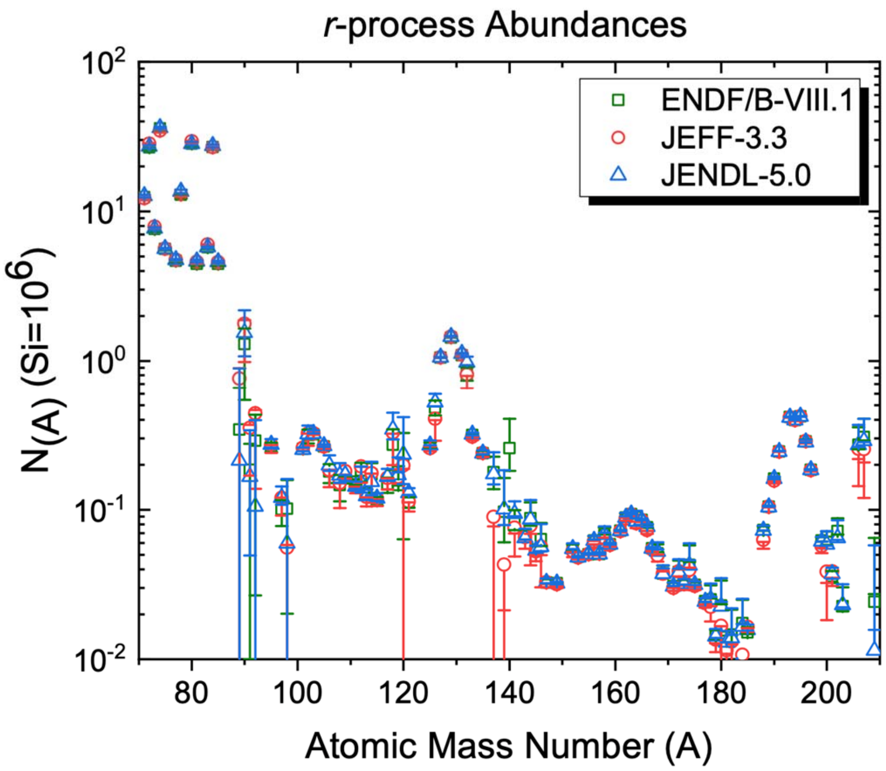

Brookhaven National Laboratory

Nuclear Structure and Stellar Abundances

- Observing the second N=82 and the third N=126 r-process peaks provides strong evidence of the existence of neutron magic numbers beyond the valley of stability.
- At the same time, the lack of the first r-process peak may indicate that N=50 is not a good quantum (magic) number for neutron-rich nuclei or neutron reaction flow changes for medium nuclei.
- We experimentally studied the island of inversion near N=20 in the last 30 years (^{32}Mg, ^{31}Na, ^{22}O, …); there are several islands predicted since the work E. K. Warburton, J. A. Becker, and B. A. Brown
- The observed synergy between nuclear astrophysics and nuclear structure physics requires additional research and close cooperation between the two communities.

PHYSICAL REVIEW C
covering nuclear physics

Highlights | Recent | Accepted | Collections | Authors | Referees | Search | Press | About | Ed

Milestone

Mass systematics for A=29–44 nuclei: The deformed A~32 region

E. K. Warburton, J. A. Becker, and B. A. Brown

Phys. Rev. C **41**, 1147 – Published 1 March 1990

An article within the collection: *Physical Review C* 50th Anniversary Milestones

Article | References | Citing Articles (594) | PDF | Export Citation

ABSTRACT

Further evidence for the presence of an anomaly in binding energies for the "island of inversion" centered at Z=11, N=21 is obtained by comparison of shell-model calculations to experiment. The calculations were done with a shell-model interaction that is applicable to nuclei with active valence nucleons in both the (1s,0d) and (0f,1p) major shells. This interaction is described in detail as are its predictions for binding energies and energy spectra of Z=8–20, N=18–25 nuclei. These calculations provide the background for the exploration of the "island of inversion." The extent of the "island" and the magnitude of the anomaly is explored by calculating the binding energies of 2ħω excitations of neutrons from the (1s,0d) shell to the (0f,1p) shell relative to the 0ħω ground state. The reason why mixed (0+2)ħω calculations are not considered reliable is addressed. Truncation schemes and a weak-coupling approximation are used to extend the range of the calculations. It is found that for Z=10–12, N=20–22 (and possibly N>22) nuclei the lowest 2ħω state is more bound than the 0ħω ground state. The role of odd n nħω excitations is considered and it is found that the 1ħω ground state always lies below that of 3ħω, and for N=19, 21, and 23, the lowest 1ħω state is in close competition with 2ħω for the lowest binding energy. Collectivity is considered via E2 observables and energy spectra for the 2ħω ground-state bands. The reason for the existence of the "island" is discussed.

Received 11 October 1989

Brookhaven National Laboratory

Takeaways

- Integral values for the five major libraries were calculated and compared with benchmarks and the EXFOR library.
- ENDF/B-VIII.1 is the best-evaluated nuclear data library for astrophysics.
- R-process abundances for ENDF/B-VIII.1, JEFF-3.3, and JENDL-5.0 have been calculated.
- Cerium evaluation (^{140}Ce) helped to improve ENDF/B; revisiting barium (^{138}Ba) cross sections is needed.

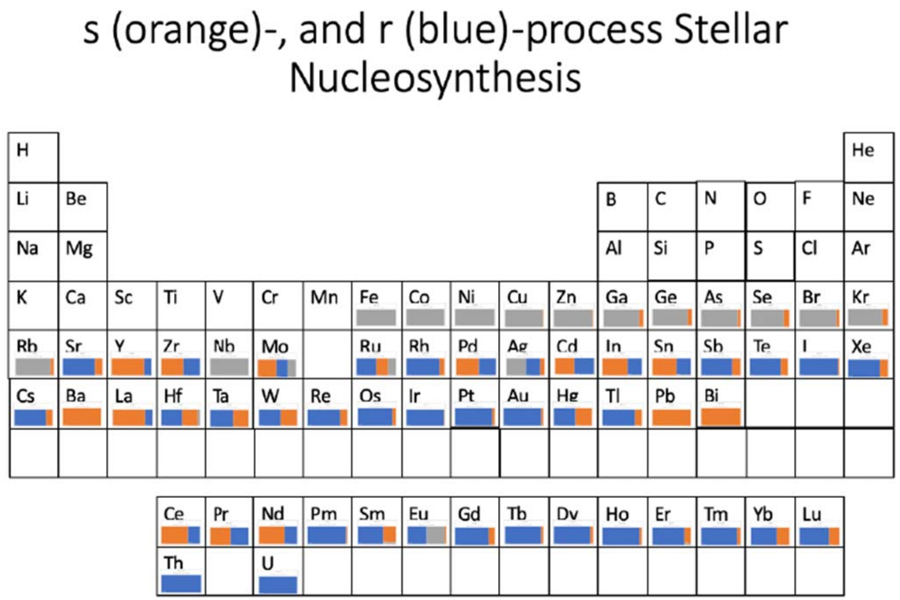

Brookhaven National Laboratory